THE JOURNAL OF PHYSICAL CHEMISTRY A

Subscriber access provided by DUKE UNIV

Article

Molecular Design of Porphyrin-Based Nonlinear Optical Materials

Shahar Keinan, Michael J. Therien, David N. Beratan, and Weitao Yang

J. Phys. Chem. A, **2008**, 112 (47), 12203-12207 • DOI: 10.1021/jp806351d • Publication Date (Web): 31 October 2008

Downloaded from http://pubs.acs.org on January 9, 2009

More About This Article

Additional resources and features associated with this article are available within the HTML version:

- Supporting Information
- Access to high resolution figures
- Links to articles and content related to this article
- Copyright permission to reproduce figures and/or text from this article

View the Full Text HTML

ACS Publications
High quality. High impact.

The Journal of Physical Chemistry A is published by the American Chemical Society. 1155 Sixteenth Street N.W., Washington, DC 20036

Molecular Design of Porphyrin-Based Nonlinear Optical Materials

Shahar Keinan, Michael J. Therien, David N. Beratan,* and Weitao Yang*

Department of Chemistry, Duke University, Durham, North Carolina 27708

Received: July 18, 2008; Revised Manuscript Received: September 13, 2008

Nonlinear optical chromophores containing (porphyrinato)Zn(II), proquinoid, and (terpyridyl)metal(II) building blocks were optimized in a library containing $\sim 10^6$ structures using the linear combination of atomic potentials (LCAP) methodology. We report here the library design and molecular property optimizations. Two basic structural types of large β_0 chromophores were examined: linear and T-shaped motifs. These T-shaped geometries suggest a promising NLO chromophoric architecture for experimental investigation and further support the value of performing LCAP searches in large chemical spaces.

Introduction

The nonlinear optical (NLO) response is employed in optical communications, signal processing, switching, limiting, and modulating devices.[1] Nonlinear materials, made from organic components, have potential advantages over inorganic structures, including lower cost, low dielectric constant, diversity of possible structures, and ultrafast response.[2,3] Discovering organic molecules with large nonlinear responses is an active pursuit. Properties are often manipulated by making structural modifications to donor and acceptor building blocks, as well as to conjugated linking π-units.[2,4] Structural modifications can include adding/removing chemical groups, interchanging heteroatoms, or manipulating conjugation, for example.[5−7] However, if one wishes to scan a large region of chemical space, one cannot directly enumerate and examine all molecular possibilities either theoretically or experimentally. Rather, one benefits from employing optimization techniques.[8]

Although continuous optimization was explored previously,[9,10] it was challenging to associate optimization results with realizable chemical structures. We recently described a linear combination of atomic potentials (LCAP) approach to transform molecular optimization, a challenge of discrete optimization, into a continuous optimization problem, without compromising the link to realizable molecular structures.[11−13] Others have applied related ideas to drug design[14−17] and protein folding.[18] A different approach was suggested by Kuzyk et al.[19,20] where a potential energy function was optimized for maximal intrinsic hyperpolarizability. This approach is similar to the early idea of optimization pursued by Kuhn and Beratan.[9] On the basis of the optimized function, a molecular target was suggested.[21] Here, we describe a version of the LCAP approach where the gradient (directing the progress of the optimization) is computed using finite-difference methods. This approach skirts exploration of rugged landscapes associated with "alchemical" species and is a general strategy for finding the most favorable solutions for various optimization problems. The approach used here resembles the "dead end elimination" algorithm[22,23] (based on the "branch and bound" algorithm) and is especially useful in discrete optimization.[24]

This study describes the use of the LCAP algorithm to search a large porphyrin-based chemical library in order to identify lead structures with promising NLO responses. The central backbone of the library is composed of the (trispyridyl)$_2$Ru ((tpy)$_2$Ru) and (porphinato)Zn(II) building blocks, that are constituents of known structures with large NLO characteristics.[25−29] This is, to the best of our knowledge, the first use of inverse design methods to improve the NLO properties of realistic organic-based NLO chromophores (beyond proof of principle demonstrations) in a class that promises particularly large electronic nonlinear response.

Methods

Computational Details. All molecular geometries were optimized with the AM1[30] semiempirical method, as implemented in MOPAC 6.0. It is important to note that while there is a low barrier to rotation of unencumbered aromatics about an ethyne bond,[28,31−36] conjugative interactions reduce the extent of condensed-phase conformational heterogeneity in these systems. If a Boltzmann-weighted distribution of torsional angles similar to that manifest for closely related conjugated structures is assumed,[28,31−36] the typical angle between (porphinato)metal-(porphinato)metal and (porphinato)metal-(terpyridyl)metal least-squares planes would be expected to be less than 50°. In our AM1 calculations, a maximally conjugated structure was assumed, given: (i) that this conformer is known to be populated for experimentally interrogated chromophores similar to those investigated computationally in the chemical library, and (ii) that it has been established that the electronic structure of these ethyne-bridged (porphinato)metal-(porphinato)metal and (porphinato)metal-(terpyridyl)metal chromophores varies little as a function of the dihedral angle between bridged (porphinato)metal and (terpyridyl)metal components, due to the cylindrical π symmetry of the ethyne moiety and the nature of the ground and excited-state wave functions of the component absorbers.[28,31−36]

For AM1 geometry optimization, Ru and Fe atoms (not parametrized in AM1) were replaced by Zn. DFT calculations (as described in the Supporting Information) show that (tpy)$_2$Zn, (tpy)$_2$Ru, and (tpy)$_2$Fe geometries are nearly identical, regardless of the metal atom. Also, computed NLO response values are not sensitive to small changes in the (tpy)$_2$metal geometry, suggesting that using Zn instead of Ru and Fe in the geometry optimization will not greatly influence the calculated values.

All electronic structure calculations were preformed with the CNDO computer code,[37] using the INDO/s semiempirical

* To whom correspondence should be addressed. E-mail: D. N. B., david.beratan@duke.edu; W. Y., weitao.yang@duke.edu.

10.1021/jp806351d CCC: $40.75 © 2008 American Chemical Society
Published on Web 10/31/2008

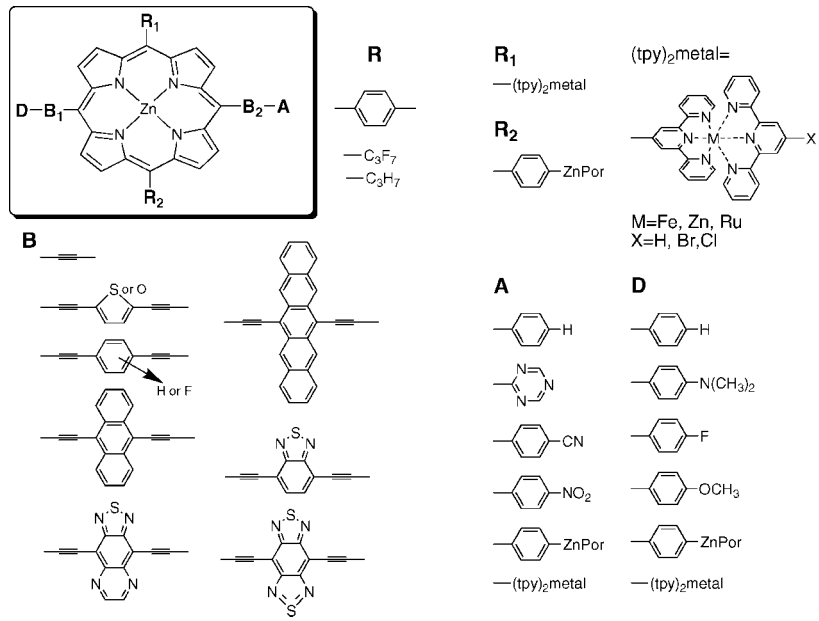

Figure 1. The molecular library for the LCAP optimization. The library contains six variable positions (**B**$_1$, **B**$_2$, **D**, **A**, **R**$_1$, **R**$_2$). There are 2 linker sites (**B**$_1$ and **B**$_2$), each with 10 possible chemical groups, a donor (**D**), and an acceptor (**A**), each with 14 possible groups, one porphyrin substituent group (**R**$_1$) with 12 possible species and a second porphyrin substituent group (**R**$_2$) with 4 possible species. The library contains 940,800 molecules.

Hamiltonian.[38] A window of 100 orbitals below and above the HOMO was used for single configuration interaction (CIS). The lowest 300 excitations from that active space were used to calculate the nonlinear optical properties. The size of the CI window and the number of excitations were chosen based on convergence tests, by expanding the CI space until the computed β_{tot} value did not change (the convergence criterion was $\pm$ 0.1 $\times$ 10^{-30} esu). Solvent was included with the Liptay/Rettig[39,40] PCM solvent model of acetonitrile (CH_3CN, dielectric constant = 36.69; refractive index = 1.344). The static (ω = 0.0 eV) hyperpolarizability, $\beta_{0,tot}$, was calculated using the Orr−Ward[41] sum-over-states method. $\beta_{0,tot}$ is defined (for w = 0) in eqs 1 and 2:[42]

$$\beta_{tot} = \sqrt{\beta_x^2 + \beta_y^2 + \beta_z^2}; \quad \left(\beta_i = \beta_{iii} + {}^1\!/_3 \sum_{j \neq i} (\beta_{ijj} + \beta_{jij} + \beta_{jji})\right) \tag{1}$$

$$\beta_{i,j,k}(-2\omega;\omega,\omega) = \sum_P \sum_{e,e'} \frac{\langle 0|i|e\rangle\langle e|j|e'\rangle\langle e'|k|0\rangle}{(E_e - E_0 - \hbar 2\omega)(E_{e'} - E_0 - \hbar\omega)} \tag{2}$$

Here, i, j, and k denote directional axes; e and e' denote excited states; and 0 is the ground state.

Optimization Algorithm. Figure 1 shows the molecular library that was used in the optimization. This library was constructed by choosing fragments from known NLO chromophores.[25−29,43] The library contains a basic (porphyrinato)Zn(II) skeleton, with six positions (**B**$_1$, **B**$_2$, **D**, **A**, **R**$_1$, **R**$_2$) that were varied. We explored structural variations of two linkers (**B**$_1$ and **B**$_2$), each with 10 member libraries, as well as a donor (**D**) and an acceptor (**A**), each with 14 member libraries. There is also one substituent (**R**$_1$) with 12 choices and a second substituent (**R**$_2$) with 4 choices. The library diversity encompasses several types of linkers, including proquinoidal[28] species and aromatic units. The central metal ion of the $(tpy)_2$metal complex was varied (metal = Zn^{2+}, Ru^{2+}, and Fe^{2+}), as was the substituent (X) on the $(tpy)_2$metal ligand. Porphyrin ligand ancillary groups were also varied in this study: meso-C_3H_7, C_3F_7, and phenyl groups were probed. The library contains 10 $\times$ 10 $\times$ 14 $\times$ 14 $\times$ 12 $\times$ 4 = 940,800 molecules.

We used the following finite difference LCAP algorithm to optimize the electronic hyperpolarizabilities. There are j = 1−6 variable positions, and n_j^i possible groups for each R_j position:

1. Begin with a random molecule **X** (randomly choosing a chemical group for each of the j = 1−6 positions)
2. Calculate β_{tot} for molecule **X** using:
   - AM1 geometry optimization
   - INDO/s CIS calculation of linear spectra
   - Sum-over-states calculation of β_0.
3. Build molecule **Y** using one of the two methods detailed in the next section. Calculate β_{tot} of molecule **Y** via:
   - AM1 geometry optimization
   - INDO/s CIS calculation of linear spectra
   - Sum-over-states calculation of β_0.

Find the species n_j^i that maximally increases β_{tot} for each position R_j.

4. Build the next molecule $\mathbf{X}_{new}$, containing all the n_j^i groups (one per R_j position) that had the largest property values.
5. Was the new molecule, $\mathbf{X}_{new}$, previously analyzed?

If **no**−go to step 2 for another cycle.

If **yes**−end optimization.

Two slightly different versions of the algorithm were used at step #3 to build the next molecule **Y**. In the first version, the optimal groups (n_j^i) for all six positions were identified and changed together, allowing improved parallelization, and escape from local maxima. In the second version, the optimal n_j^i group for position R_j was found and changed in the same step, so that each step improves on the previous one (resembling a "branch and bound" algorithm). Using both versions allows a more comprehensive scan of the molecular surface.[24] Note that results found here were not particularly dependent on the specific algorithm used.

TABLE 1: Porphyrin-Based, Large β_0 Chromophores Found in 10 Runs of the LCAP Algorithm[a]

no. of runs	name	β_0 [$\times 10^{-30}$ esu]
2	LPor_T1	9712
3	LPor_T2	8403
1	LPor_L1	4484
1	LPor_L2	3246
1	LPor_L3	3757
2	LPor_L4	3770

[a] Geometries were optimized with AM1, β was calculated using INDO/s CIS (100, 100) and the acetonitrile PCM model.

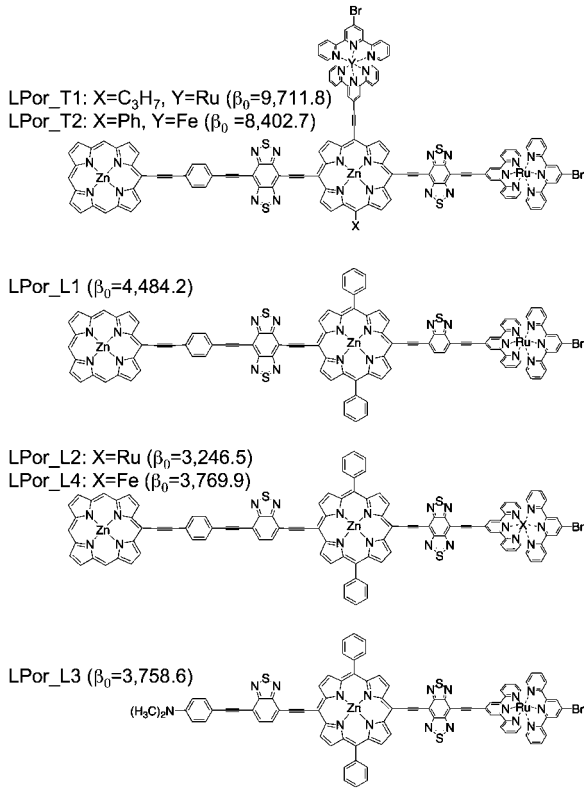

Figure 2. Structures of the six largest β NLO chromophores found in the 10 LCAP optimization runs. β_0 is in units of 10^{-30} esu.

Results and Discussion

There were 10 discrete LCAP optimization runs, with an average of 5.2 steps per run. The number of steps is equal to how many times a new molecule $\mathbf{X}_{\mathbf{new}}$ was produced and tested (step #4 in the algorithm). Table 1 and Figure 2 summarize the results of the runs, displaying the optimized structures and their respective NLO properties. Figure 3 shows an example of two optimization trajectories.

We have found two groups of large β_0 chromophores in the LCAP optimization: linear and T-shaped structures. Both groups contain the $(tpy)_2$metal-proquinoidal-(porphyrinato)Zn(II) linear motif, and most structures (9 out of 10) contain the larger $(tpy)_2$metal-proquinoidal-(porphyrinato)Zn(II)-proquinoidal-phenyl- (porphyrinato)Zn(II) linear structure. In the T-shaped geometries, the second $(tpy)_2$metal group is bound to the central (porphyrinato)Zn(II) via an ethynyl bridge at an adjacent macrocycle meso position. The T-shape chromophores present a new molecular realization of this structural motif for potentially large hyperpolarizability chromophores with β_0 estimated 9000×10^{-30} esu.

Proquinoidal groups linked to the (porphyrinato)Zn(II) meso position via an ethynyl bridge have unusually large quinoidal

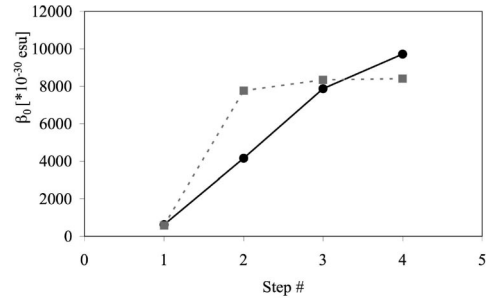

Figure 3. Two characteristic optimization trajectories. In the first optimization (black circles), the random seed structure has $\beta_0 = 616$; after 5 steps LPor_T1 ($\beta_0 = 9{,}712$) is found. In the second optimization trajectory (gray squares), the random seed structure has $\beta_0 = 572$; after 5 steps LPor_T2 ($\beta_0 = 8{,}403$) is found. β_0 is in units of 10^{-30} esu.

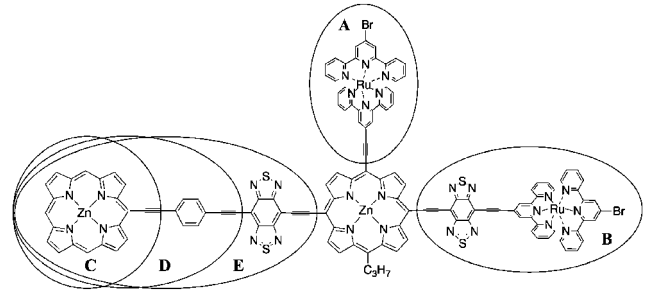

Figure 4. Structural variants of LPor_T1. These modifications include: I. Changing the central atom of the $(tpy)_2$Ru moiety A from Ru to Zn; II. Changing the central atom of the $(tpy)_2$Ru moiety B from Ru to Zn; III. Changing the Br atom to H on the $(tpy)_2$Ru moiety A; IV. Changing the Br atom to H on the $(tpy)_2$Ru moiety B; V. Removing the $(tpy)_2$Ru moiety A; VI. Removing the $(tpy)_2$Ru moiety B; VII. Removing the (porphyrinato)Zn(II) moiety C; VIII. Removing the (porphyrinato)Zn(II) moiety C and the phenyl group D; and IX. Removing the (porphyrinato)Zn(II) moiety C, phenyl D and proquinoidal unit E.

TABLE 2: Calculated β_0 Values for Structural Variants of LPor_T1[a]

	β_0 [$\times 10^{-30}$esu]	% of LPor_T1 (%)
LPor_T1	9712	100
I. Ru(A) → Zn(A)	9040	93
II. Ru(B) → Zn(B)	9129	94
III. Br(A) → H(A)	8960	92
VI. Br(B) → H(B)	8795	90
V. Remove A	2667	27
VI. Remove B	1479	15
VII. Remove C	2265	23
VIII. Remove C + D	1152	12
IX. Remove C + D + E	397	4

[a] Geometries were optimized with AM1, $\beta 0$ was calculated with INDO/s CIS (100 100), and the acetonitrile PCM model was used.

resonance contribution to the low-lying electronically excited singlet states of these species. This significantly red-shifts the corresponding Q-state absorption, relative to that seen for the ethynyl-(porphyrinato)Zn(II) benchmark, up to 1100nm (1.1 eV), vida infra.[28] For example, the spectrum of (porphyrinato)Zn(II)-proquinoid-(porphyrinato)Zn(II), PZnE_BBTD_EPZn, features a broad, intense Q-band at 1006 nm and characteristic B band absorption maxima at 479 and 429 nm.[28] These characteristics were attributed to lowering the energy of a highly stabilized proquinoid-located LUMO. The same features are found in the structures that were optimized with the LCAP algorithm. For example, the calculated excitations for LPor_T1 show a strong, broad Q-band at 1339 nm and B-band transitions that span the 400−500 nm regime, resembling experimental observations for the similar, but shorter, PZnE_BBTD_EPZn structure.[28]

TABLE 3: λ_{max}, Calculated for Strongest Transition, Oscillator Strength (f_{ge}), and the Dipole Moments Differences ($\Delta\mu_{ge}$) for Several of the Structural Variants of LPor_T1[a]

	λ_{max} (nm)	E_{ge} [eV]	f_{ge}	$\Delta\mu_{ge}$ [Debye]	$f_{ge}\Delta\mu_{ge}/E_{ge}^3$	β_0 [$\times 10^{-30}$ esu]	HOMO	LUMO
LPor_T1	1339	0.92	3.1	17.3	68.9	9712	(porphyrinato) Zn(II) B	proquinoidal E + (porphyrinato)Zn(II) B + $(tpy)_2$Ru A
II. Ru(B) → Zn(B)	1326	0.93	3.0	16.6	61.9	9129	(porphyrinato) Zn(II) B	proquinoidal E + (porphyrinato)Zn(II) B + $(tpy)_2$Ru A
VI. Remove B	1012	1.22	1.8	4.8	4.8	1479	(porphyrinato) Zn(II) B	$(tpy)_2$Ru A
VIII. Remove C + D	1072	1.16	1.9	5.5	6.7	1152	proquinoidal adjunct to (porphyrinato)Zn(II) B	proquinoidal E

[a] Also shown are the full β_0 (eq 2), and the spatial location of the HOMO and LUMO.

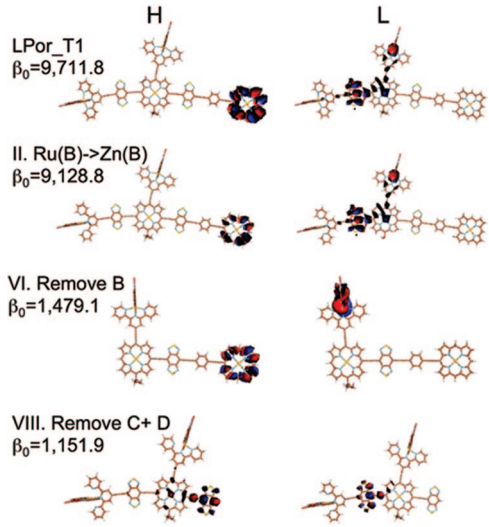

Figure 5. INDO/s calculated HOMOs and LUMOs for LPor_T1 and subset of its structural derivatives probed in this study. β_0 is in units of 10^{-30} esu. [48]

In order to investigate the origins of the large NLO response of LPor_T1, we tested several structural modifications to the LPor_T1 core structure (Figure 4 and Table 2). These modifications included changing the central metal of the tpy_2(metal) complex, changing Br to H, and removing substituents of the (porphyrinato)Zn(II) central ring. For each new structure, the geometry was optimized with AM1, and β_0 computed. Removing one of the three "arms" of the T (either one of the two $(tpy)_2$Ru units or a (porphyrinato)Zn(II)) lowers β_0 dramatically, indicating the importance of the composite supermolecule for the NLO response. Changing the metal atom in the $(tpy)_2$metal did not dramatically change β_0. However, changing Br to H on the external $(tpy)_2$metal group lowered β_0 by 10%. This effect arise from the higher electronegativity of Br, which stabilized the orbital on that (porphyrinato)Zn(II) ring.

An approximate strategy to evaluate the contribution of structural elements to the NLO response is to use a two-states model, eq 3:

$$\beta_{2-\text{state}} \propto \frac{\mu_{ge^2}\Delta\mu_{ge}}{E_{ge}^{\ 2}} \propto \frac{f_{ge}\Delta\mu_{ge}}{E_{ge}^{\ 3}} \qquad (3)$$

The response properties can be tuned by varying the energy difference between the ground and excited state (E_{ge}), the transition moment (μ_{ge}), and the difference in dipole moments between the two states ($\Delta\mu_{ge}$). The two-state model is a simplification, since it neglects the multitude of excited states that contribute to β.[44] However, it is a useful model for understanding electronic structure effects on β. Table 3 shows the contributors to the 2-state values for some of the LPor_T1 derivatives, and Figure 5 plots the INDO/s HOMOs and LUMOs for these derivatives.

Several useful conclusions can be drawn from Table 3. In the chromophores studied here, strong NLO characteristics arise from all three different contributors to $\beta_{2\text{-state}}$. LPor_T1 has a 3-fold larger $\Delta\mu_{ge}$ than the same chromophore after removing (porphyrinato)Zn(II) moiety C and the phenyl group D (VIII), and the same effect is evident when comparing the strongest excitation λ_{max}, and the transition dipole moment, μ_{ge}. The combination of low energy and strong transition dipole, as well as large dipole moment changes upon excitation contribute to the large response observed in the T-shaped chromophores. The electron density of the frontier orbitals indicates the localization of the donor (HOMO) and acceptor (LUMO) states, Figure 5. In LPor_T1, the donor is located on the (porphyrinato)Zn(II) B, and the acceptor is spread over the central (porphyrinato) Zn(II), proquinoidal linker (C unit) and $(tpy)_2$Ru (A unit), which explains the observed large decrease in the NLO response upon the removal of A, B, or C.

Branched NLO chromophores (such as Λ-shaped structures) were studied recently, using both experimental[45] and computational[46] approaches, in the hope of building phase-matched second-harmonic generation crystals. Branched chromophores may have the ability to overcome the antiparallel packing problem of linear chromophores, as well as to provide enhanced transparency (since branched NLO chromophores lack the nonlinearity-transparency tradeoff of 1D chromophores[46]). These chromophores were shown to have two degenerate charge-transfer excited states ($D_1^+D_2A^-$ and $D_1D_2^+A^-$) lying close in energy, each providing a contribution to β with the same sign. The T-shaped chromophores we examined in this contribution employ the same structural logic, with two acceptors ($(tpy)_2$Ru) and a donor ((porphyrinato)Zn(II)) connected through a second porphyrin. Kuzyk and Watkins investigated the effects of geometry on hyperpolarizability with potential energy functions that are given by a superposition of charged components ("force centers"), representing atomic nuclear charges, that lie in various planar geometrical arrangements.[47] They found that for certain specific geometries, such as the T (or λ) geometries, the hyperpolarizability is near the fundamental available limit. They showed that the fundamental limiting values can be obtained for a geometry that has two identical donor groups on one side of the molecule and an acceptor group on a third prong, with the acceptor along a symmetry axis between the two donors. These are exactly the kinds of T-shaped chromophores obtained in our LCAP optimizations.

Conclusions

We have identified favorable T-shaped porphyrin-based NLO chromophores from a molecular library containing 940 800 available compounds by the LCAP optimization. T-shaped

chromophores have an acceptor and two donor moieties arranged around a central (porphyrinato)Zn(II) unit, and all of these groups are shown to contribute to the large β_0 values. These chromophores are predicted to display low-energy excited states and strong optical transitions in the range of 1000−1300 nm (due to the proquinoidal linkers). Also, strong differences in the dipole moments between the ground and the excited states contribute to the enhancement of the NLO response. These new structures suggest many new directions to explore in the synthesis and characterization of novel NLO structures. With this demonstration, NLO chromophore design joins earlier examples of LUMO engineering[12] and redox potential engineering[49] to illustrate the utility of the LCAP approach.

Acknowledgment. We thank Prof. Jeffery R. Reimers for providing the CNDO program and the DARPA Predicting Real Optimized Materials project through ARO (W911NF-04-1-0243) for support. This work was supported in part by the National Center for Supercomputing Applications under Grant No. TG-CHE070006N and utilized the TeraGrid NCSA Tungsten machine.

Supporting Information Available: Data comparing geometries of three different metals in $(tpy)_2$metal units, calculated with DFT and INDO/s methods.This material is available free of charge via the Internet at http://pubs.acs.org.

References and Notes

(1) Dalton, L. R. *J. Phys.: Condens. Matter* **2003**, *15*, R897.
(2) *Molecular Nonlinear Optics-Materials, Physics and Devices*; Zyss, J., Ed.; Academic Press: San Diego, CA, 1994.
(3) van der Boom, M. E. *Angew. Chem., Int. Ed.* **2002**, *18*, 3363.
(4) *Nonlinear Optical Materials: Theory and Modeling*; Karna, S. P., Yeates, A. T., Eds.; ACS: Washington, D.C., 1996; Vol. 628.
(5) Beratan, D. N. In *Materials for Nonlinear Optics: Chemical Perspective*; Marder, S. R., Sohn, J. E., Stucky, G. D., Eds.; ACS: Washington, D.C., 1991; Vol. 455; pp 89.
(6) Keinan, S.; Ratner, M. A.; Marks, T. J. *Chem. Phys. Lett.* **2006**, *417*, 293.
(7) Zhu, P.; Kang, H.; Facchetti, A.; Evmenenko, G.; Dutta, P.; Marks, T. J. *J. Am. Chem. Soc.* **2003**, *125*, 11496.
(8) *Directing Matter and Energy: Five Challenges for Science and the Imagination*; Hemminger, J., Fleming, G., Ratner, M. A. , Eds.; U. S. Department of Energy, 2007. On the web: http://www.sc.doe.gov/bes/reports/list.html.
(9) (a) Kuhn, C.; Beratan, D. N. *J. Phys. Chem.* **1996**, *100*, 10595. (b) Risser, S. M.; Beratan, D. N.; Marder, S. R. *J. Am. Chem. Soc.* **1993**, *115*, 7719.
(10) Franceschetti, A.; Zunger, A. *Nature* **1999**, *402* (6757), 60.
(11) Wang, M.; Hu, X.; Beratan, D. N.; Yang, W. *J. Am. Chem. Soc.* **2006**, *128*, 3228.
(12) Keinan, S.; Hu, X. Q.; Beratan, D. N.; Yang, W. T. *J. Phys. Chem. A* **2007**, *111*, 176.
(13) (a) Xiao, D.; Beratan, D. N.; Yang, W. *J. Chem. Phys.* **2008**, *129*, 044106. (b) Hu, X.; Beratan, D. N.; Yang, W. *J. Chem. Phys.* **2008**, *129*, 064102.
(14) von Lilienfeld, O. A.; Lins, R. D.; Rothlisberger, U. *Phys. Rev. Lett.* **2005**, *95*, 153002.
(15) von Lilienfeld, O. A.; Tuckerman, M. E. *J. Chem. Phys.* **2006**, *125*, 154104.
(16) von Lilienfeld, O. A.; Tuckerman, M. *J. Chem. Theory Comp.* **2007**, *3*, 1083.
(17) Marcon, V.; von Lilienfeld, O. A.; rienko, D. *J. Chem. Phys.* **2007**, *127*, 064305.
(18) Koh, S. K.; Ananthasuresh, G. K.; Vishveshwara, S. *Int. J. Rob. Res.* **2005**, *24*, 109.
(19) Zhou, J.; Kuzyk, M. G.; Watkins, D. S. *Opt. Lett.* **2006**, *31*, 2891.
(20) Zhou, J.; Szafruga, U. B.; Watkins, D. S.; Kuzyk, M. G. *Phys. Rev. A* **2007**, *76*, 053831.
(21) Pérez-Moreno, J.; Zhao, Y.; Clays, K.; Kuzyk, M. G. *Opt. Lett.* **2007**, *32*, 59.
(22) Schrijver, A. *Theory of Linear and Integer Programming*; J. Wiley and Sons: New York, 1998.
(23) Gordon, D. B.; Mayo, S. L. *J. Comput. Chem.* **1999**, *19*, 1505.
(24) Balamurugan, D.; Yang, W.; Beratan, D. N. *J. Chem. Phys.* 2008, in press.
(25) Uyeda, H. T.; Zhao, Y.; Wostyn, K.; Asselberghs, I.; Clays, K.; Persoons, A.; Therien, M. J. *J. Am. Chem. Soc.* **2002**, *124*, 13806.
(26) Zhang, T.-G.; Zhao, Y.; Asselberghs, I.; Persoons, A.; Clays, K.; Therien, M. J. *J. Am. Chem. Soc.* **2005**, *127*, 9710.
(27) Priyadarshy, S.; Therien, M. J.; Beratan, D. N. *J. Am. Chem. Soc.* **1996**, *118*, 1504.
(28) Susumu, K.; Duncan, T. V.; Therien, M. J. *J. Am. Chem. Soc.* **2005**, *127*, 5186.
(29) Duncan, T. V.; Rubtsov, I. V.; Uyeda, H. T.; Therien, M. J. *J. Am. Chem. Soc.* **2004**, *126*, 9474.
(30) Dewar, M. J. S.; Zoebisch, E. G.; Healy, E. F.; Stewart, J. P. P. *J. Am. Chem. Soc.* **1985**, *107*, 3902.
(31) Lin, V. S.-Y.; DiMagno, S. G.; Therien, M. J. *Science* **1994**, *264*, 1105.
(32) Lin, V. S.-Y.; Therien, M. J. *Chem.-Eur. J.* **1995**, *1*, 645.
(33) Susumu, K.; Therien, M. J. *J. Am. Chem. Soc.* **2002**, *124*, 8550.
(34) Rubtsov, I. V.; Susumu, K.; Rubtsov, G. I.; Therien, M. J. *J. Am. Chem. Soc.* **2003**, *125*, 2687.
(35) Duncan, T. V.; Song, K.; Hung, S.-T.; Miloradovic, I.; Persoons, A.; Verbiest, T.; Therien, M. J.; Clays, K. *Angew. Chem., Int. Ed. Engl.* **2008**, *47*, 2978.
(36) Duncan, T. V.; Ghoroghchian, P. P.; Rubstov, I. V.; Hammer, D. A.; Therien, M. J. *J. Am. Chem. Soc.* **2008**, *130*, 9773.
(37) Zeng, J.; Hush, N. S.; Reimers, J. R. *J. Am. Chem. Soc.* **1996**, *118*, 2059.
(38) Ridley, J.; Zerner, M. *Theor. Chim. Acta* **1973**, *32*, 111.
(39) Liptay, W. PCM Model. In *Modern Quantum Chemistry*; Sinanoğlu, O., Ed.; Academic Press: New York, 1965; Vol. III; pp 45.
(40) Rettig, W. *J. Mol. Struct.* **1982**, *84*, 303.
(41) Orr, B. J.; Ward, J. F. *Mol. Phys.* **1971**, *20*, 513.
(42) Willetts, E.; Rice, J. E.; Burland, D. M.; Shelton, D. P. *J. Chem. Phys.* **1992**, *97*, 7590.
(43) Xu, T.; Wu, S. P.; Miloradovic, I.; Therien, M. J.; Blasie, J. K. *Nano Lett.* **2006**, *6*, 2387.
(44) Nguyen, K. A.; Day, P. N.; Pachter, R.; Tretiak, S.; Chernyak, V.; Mukamel, S. *J. Phys. Chem. A.* **2002**, *106*, 10285.
(45) Moylan, C. R.; Ermer, S.; Lovejoy, S. M.; McComb, I. H.; Leung, D. S.; Wortmann, R.; Krdmer, P.; Twieg, R. J. *J. Am. Chem. Soc.* **1996**, *118*, 12950.
(46) Yang, M.; Champagne, B. *J. Phys. Chem. A* **2003**, *107*, 3942.
(47) Kuzyk, M. G.; Watkins, D. S. *J. Chem. Phys.* **2006**, *124*, 244104.
(48) Schaftenaar, G.; Noordik, J. H. *J. Comput.-Aided Mol. Des.* **2000**, *14*, 123.
(49) Keinan, S.; Paquette, W. D.; Skoko, J. J.; Beratan, D. N.; Yang, W.; Shinde, S.; Johnson, P. A.; Lazso, J. S.; Wipf, P. *Org. Biomol. Chem.* **2008**, *6*, 3256.

JP806351D